A Miniaturized Glucocorticoid Receptor Translocation Assay Using Enzymatic Fragment Complementation Evaluated with qHTS

Ping Jun Zhu[1], Wei Zheng[1], Douglas S. Auld[1], Ajit Jadhav[1], Ryan MacArthur[1], Keith R. Olson[2], Kun Peng[2], Hyna Dotimas[2], Christopher P. Austin[1] and James Inglese[*,1]

[1]*National Institutes of Health, National Human Genome Research Institute, NIH Chemical Genomics Center, 9800 Medical Center Drive, MSC: 3370, Bethesda, MD 20892-3370, USA*

[2]*DiscoveRx Inc., Fremont, CA, USA*

Abstract: Nuclear translocation is an important step in glucocorticoid receptor (GR) signaling and assays that measure this process allow the identification of nuclear receptor ligands independent of subsequent functional effects. To facilitate the identification of GR-translocation agonists, an enzyme fragment complementation (EFC) cell-based assay was scaled to a 1536-well plate format to evaluate 9,920 compounds using a quantitative high throughput screening (qHTS) strategy where compounds are assayed at multiple concentrations. In contrast to conventional assays of nuclear translocation the qHTS assay described here was enabled on a standard luminescence microplate reader precluding the requirement for imaging methods. The assay uses β-galactosidase α complementation to indirectly detect GR-translocation in CHO-K1 cells. 1536-well assay miniaturization included the elimination of a media aspiration step, and the optimized assay displayed a Z' of 0.55. qHTS yielded EC_{50} values for all 9,920 compounds and allowed us to retrospectively examine the dataset as a single concentration-based screen to estimate the number of false positives and negatives at typical activity thresholds. For example, at a 9 μM screening concentration, the assay showed an accuracy that is comparable to typical cell-based assays as judged by the occurrence of false positives that we determined to be 1.3% or 0.3%, for a 3σ or 6σ threshold, respectively. This corresponds to a confirmation rate of ~30% or ~50%, respectively. The assay was consistent with glucocorticoid pharmacology as scaffolds with close similarity to dexamethasone were identified as active, while, for example, steroids that act as ligands to other nuclear receptors such as the estrogen receptor were found to be inactive.

Keywords: qHTS, HTS, EFC, PubChem, glucocorticoid receptor, nuclear translocation, suspension cells.

INTRODUCTION

The glucocorticoid receptor (GR, NR3C1) is a member of the nuclear receptor family of ligand-dependent transcription factors. Nuclear receptors have a modular structure consisting of a ligand-binding domain (LBD) and a DNA-binding domain (DBD). Upon binding of ligands, GR translocates from the cytoplasm to the nucleus [1, 2]. The GR-ligand complex within the nucleus binds as a dimer to specific DNA recognition sequences, glucocorticoid response elements, and co-regulator proteins that lead to either enhancement or suppression of gene transcription from a wide variety of glucocorticoid-responsive genes [3]. In addition to their important roles in normal physiology and metabolism, glucocorticoids are administered as treatments for a wide variety of allergic, autoimmune, and neoplastic conditions and thus GR has been a valuable target for drug development [4-8].

A number of nuclear receptor assay formats have been devised for HTS [9]. For enabling the identification of selective GR ligands such assays include radiometric and fluorometric ligand-binding assays using purified GR-LBD [10-12], GR translocation assays and GR transcriptional reporter gene assays [13, 14]. As translocation may be an important

intervention point in the regulation of GR function, there is increasing interest in studying GR translocation and developing new assays that are able to monitor translocation in a cellular environment.

In the absence of its ligand, the GR is sequestered to the cytoplasm where it is associated with the heat shock protein Hsp90 [15, 16]. In the presence of its cognate ligands, GR becomes activated after induction of HDAC6 acetylation of the Hsp90 [17-19]. Interestingly, a reduction in GR translocation may be responsible for glucocorticoid resistance in a subgroup of asthma patients [20, 21]. Thus, analysis of events involved in GR translocation may lead to discovery of non-steroidal small molecules capable of more effectively modulating GR activity, highlighting the importance of cell-based assays and the use of the full-length NHR protein.

Nuclear translocation is an event common to ligands that either enhance or repress gene transcription [2]. Therefore, assays that measure translocation enable the identification of both agonists and antagonists in a single assay format. To date, high-content assays have been the method of choice for measuring translocation [22, 23]. Immunocytochemical staining is commonly used for constructing nuclear translocation assays. However, such formats are not suitable for high throughout screening due to the multiple reagent additions, cell permeabilization and washing steps required. Alternatively, translocation can be monitored by fusing autofluorescent proteins such as GFP to the protein of interest. We recently applied such an assay to measure translocation of GR in a 1536-well assay system using laser-based mi-

*Address correspondence to this author at the National Institutes of Health, National Human Genome Research Institute, NIH Chemical Genomics Center, 9800 Medical Center Drive, MSC: 3370, Bethesda, MD 20892-3370, USA; E-mail: jinglese@mail.nih.gov
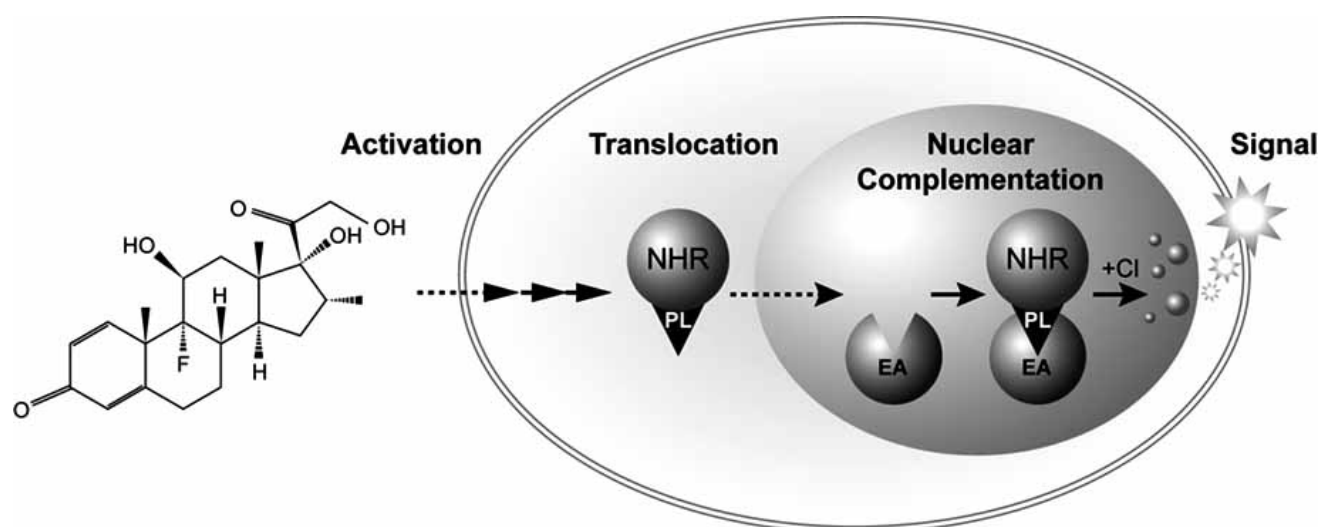
Fig. (1). EFC Assay Principle for Nuclear Translocation Using Positional Complementation. The positional complementation assay utilizes differential expression in separate cellular compartments of the EA and ProLabel (PL) components of the β-galactosidase complementation technology. One version of this assay monitors nuclear translocation of targets such as nuclear hormone receptors (NHR) without the need for antibodies, GFP or imaging. In this approach, the EA fragment of β-galactosidase is expressed exclusively in the nucleus in a parental clonal cell line. An NHR protein, such as glucocorticoid receptor, is fused to the small ProLabel peptide and expressed in the cytoplasm. When appropriately stimulated with agonist, the NHR target will translocate to the nucleus, the two fragments of β-galactosidase will complement, and a signal will be generated using a chemiluminescent substrate (Cl) for the β-galactosidase enzyme.

croplate cytometry to enumerate GFP positive nuclei [24]. However, concerns are sometimes raised in GFP-based systems due to the need to express sufficient amounts of the GR-GFP fusion protein for efficient imaging, which may in some cases interfere with particular pathways [25].

Recently, α-complementation-based assays for nuclear translocation have been described [26, 27]. A GR translocation assay designed for HTS has been developed by DiscoveRx (Fremont, CA) using enzymatic fragment complementation (EFC) of β-galactosidase, an α-complementation technology used widely for configuring various HTS assays [28] (Fig. **1**). This assay uses β-galactosidase as an indicator of GR-translocation in engineered CHO-K1 cells. The *enzyme acceptor* (EA) fragment of β-galactosidase resides in the nucleus, as designed through the use of a proprietary set of sequence modifications [29, 30]. The small peptide *enzyme donor* (ED, ProLabel) fragment of β-galactosidase is fused directly to the C-terminus of GR[§], and is localized in the cytoplasm in the absence of receptor signaling. Upon binding to a GR ligand, the complex translocates to the nucleus, where intact enzyme activity is reconstituted by complementation. The β-galactosidase activity is then detected *via* conversion of a chemiluminescent substrate.

To validate this assay we used a compound collection that included known glucocorticoids. The compound collection was screened using quantitative HTS (qHTS) where compounds are screened at seven to fifteen concentrations [31]. We describe here the optimization of this GR-EFC assay to provide a homogenous 1536-well plate assay using freshly prepared cell suspensions and the use of qHTS re-

sults to evaluate the accuracy and the sensitivity of this novel assay format.

MATERIALS AND METHODS

Materials. Two types of Kalypsys plates (San Diego, CA) were used in this study. 1536-well white solid plates were used as assay plates and 1536-well polypropylene clear plates were used as compound plates.

Compound Library. A set of 9,920 compounds were obtained from different sources including Sigma-Aldrich (LOPAC; 1280), Tocris (979), Timtec (280), Preswick (1115), Pharmacopia (3000), NCI (1979), Boston University CMLD (718), University of Pittsburgh CMLD (474), and University of Wisconsin (95). Some of these are the known pharmacologically active compounds which were used to evaluate assay performance. The LOPAC, Tocris, Timtec and Prestwick libraries were prepared in fourteen concentrations as 1:2.236 serial dilutions in DMSO in 384-well plates, and subsequently reformatted into 1536-well plates. The remaining compounds were serially diluted to seven concentrations in 1:5 ratio (for details, see Inglese *et al.* 2006). The compound archive concentrations in 1536-well plates ranged from 0.3 µM to 10 mM.

Cell Culture. Clonally derived CHO-K1 cells stably expressing NLS-enzyme acceptor fragment (EA) of β-galactosidase and GR-enzyme donor (ED) fragment of β-galactosidase (ProLabel fragment fused at C-terminal of GR) were maintained in F-12 medium (Invitrogen, Carlsbad, CA) containing 10% FBS, 2 mM L-glutamine, 50 U/ml penicillin and 50 µg/ml streptomycin, and 250 µg/ml hygromycin B, 500 µg/ml G418 (Invitrogen) at 37°C under a humidified atmosphere containing 5% CO_2 and 95% air.

EFC Detection Assay. The GR-translocation was measured by β-galactosidase activity using the PathHunter Detec-

---

[§] In transient transfection experiments, GR Prolabel fusions from GR expression vectors with Prolabel at either the C- or N-terminus gave similar expression levels and stimulation with dexamethasone (K. Olson, unpublished result).

tion Kit (DiscoveRx, Fremont, CA). The kit contains β-galactosidase substrate reagents. The 1X working solution consists of 1 part substrate and 19 parts lysis buffer prepared according to the manufacturer's protocol (DiscoveRx, Fremont CA).

Instrumentation. The flying reagent dispenser (FRD, Aurora Discovery, San Diego, CA) was used for reagent dispensing [32]. Pintool (Kalypsys, San Diego, CA) was used for compound transfer [33], with pin slot set for 1 to 200 dilution. Final DMSO (dimethyl sulfoxide) concentration was less than 0.5%. Chemiluminescence signal was measured on a ViewLux (PerkinElmer, Wellesley, MA) with measurement time 20 s and 4X binning.

HTS Assay Protocol. The assay protocol is described stepwise in Table **1**. CHO-K1 cells were detached with trypsin after reaching 85% confluency. Trypsin-containing media were removed by centrifugation; cells were re-suspended with 1% FBS F12 medium without antibiotics (antibiotics are optional at this stage) and subsequently dispensed at a density of 10^3 cells/well in 1536-well assay plates. Compounds were added and incubated for 2 h at 37°C before 1.25 µL per well of β-galatosidase substrate reagents were added. Data were collected using ViewLux after 60 min incubation at room temperature.

Data Analysis. All values are expressed as mean ± SD. The screening results were analyzed using Genedata AG (Waltham, MA). A four parameter Hill equation was fitted to the concentration-response (CR) data by minimizing the residual error between the modeled and observed responses. Outliers were masked if the difference with the modeled Hill equation exceeded the noise in the assay that was calculated from the standard deviation of the activity at the lowest tested compound concentration. Additionally, data from higher concentrations were preferentially masked if doing so

allowed the fit of the lower-concentration data to achieve significance as judged by efficacy and R^2 requirements. The CR curves were then classified based as belonging to one of four classes based on efficacy (response magnitude), presence of asymptotes, and goodness of fit of the curve to the data (R^2) [31]. These classes were (1) complete response curves containing upper and lower asymptotes, (2) incomplete response curves having an upper asymptote, (3) poorly fit curves to activity present only at the highest tested concentration, and (4) inactive, where activity was below 28.6% (3σ for the present assay) [31]. To represent the data concentration-response curves were plotted using Prism (GraphPad Software, San Diego, CA) or OriginPro (OriginLab Corp., Northhampton, MA). The Z' factor, an index for assay quality control [34], was determined by

$$Z'=1-(3*SD_{high}+3*SD_{low})/(Mean_{high}-Mean_{low})$$

False positive and false negative prevalence analysis was performed by comparing the titration-based qHTS results with single-concentration (1.8 µM and 9 µM) data derived from the qHTS dataset and applying typical hit-thresholds of either 3σ or 6σ. Single concentration hits using either threshold were then compared to the CR curves from the qHTS to determine false positives and false negatives using the following definitions:

Eq. 1. Actives = TP + FN

where TP = true positives; Compounds in the hit lists that showed high confidence CR curves in the qHTS (Class 1 and 2; see [34]). Alternatively, the low confidence CR curves (class 3) can be included in this analysis.

FN = false negatives; high confidence CR curves (Class 1 and 2) in the qHTS that were not found as positives in the hit lists.

Table 1.   GR-EFC 1536-Well Plate Assay Protocol

Step	Parameter	Value	Description
1	Reagent	5 µL	GR-CHO-K1 cells, 1000 cells per well
2	Library Compounds	23 nL	46 µM - 0.5 nM dilution series
3	Controls	23 nL	100 nM dexamethasone final concentration
4	Time	120 min	37°C and 5% CO_2,
5	Reagent	1.25 µL	Substrate buffer
6	Time	60 min	RT incubation
7	Output	20 s	ViewLux detector; clear filter
Notes			
1	The line stably expressing NLS-enzyme acceptor fragment (EA) of β-galactosidase and GR-enzyme donor (ED) fragment of β-galactosidase. The cells were maintained with F12 medium in the presence of hygromycin B and G418. Cells added with FRD to 1536-well white solid plates and covered with Kalypsys stainless steel gasket-containing plate lids with gas-exchange holes.		
2	Pin-tool compound transfer was performed directly after cell seeding.		
3	Positive control; Pin-tool transfer.		
4	Standard cell culture incubation conditions.		
5	Substrate buffer diluted 1:5 in final reaction. Added with FRD.		
7	4x binning.		

Eq. 2. Inactives = FP +TN

where FP = false positives; compounds in the hit lists that were found to be inactive in the qHTS (Class 4).

TN = true negatives; compounds not found in the hit list that were inactive in the qHTS.

In this manner the so-called "truth table" [35, 36] containing the numbers of TP, FP, FN and TN could be fully populated for the 3σ and 6σ hit cutoffs.

RESULTS

Assay optimization. For 1536-well format we have developed a 'mix-and-read' protocol and to shorten assay cycle time, we used cell suspensions to perform the EFC-GR screen. To define the optimal assay time, cells were cultured for a variety of times before adding the selective GR agonist, dexamethasone. The signal to background (S/B) ratio was observed to be 4-fold for the assay using freshly prepared cell suspensions. Increases in incubation time showed no clear effect on S/B ratio, although overnight culture of the cells resulted in a 6-fold S/B ratio (Fig. **2A**), however this signal improvement would be offset by a significant increase in assay time, a parameter we aimed to minimize.

In the originally described 384-well format EFC-GR translocation assay, after overnight culture, the medium is replaced with serum-free medium prior to the assay [26]. However an important consideration in the adaption of 384-well cell-based assays to a 1536-well format is the removal or minimization of media aspiration steps. To determine the minimum serum concentration acceptable, we performed the assay with concentrations of serum varying from 1-10%. High serum concentrations lead to reduction in the absolute value of the luminescence signal (Fig. **2B**), but had no effect on the S/B ratio (Fig. **2C**). Given these results and to minimize compound protein binding, 1% FBS was used in the final optimized 1536-well assay used for qHTS.

The effect of cell density on the EFC-GR assay was also examined by measuring the CR curves for the positive control dexamethasone at various cell densities (Fig. **3**). Overall, the EC_{50} values showed no effect at the three tested cell densities (500, 1000 and 2000 per well) using overnight cultures. However, EC_{50} values from overnight culture were slightly higher than that from freshly suspended cells. In addition, absolute values of luminescence signal from the freshly prepared cell suspension were higher than that from the overnight culture. To balance the cell culture requirements while maintaining a strong luminescence signal output, we chose 1000 cells/well for this protocol. The final optimized assay protocol is shown in Table **1**.

Assay validation and qHTS. qHTS was performed by using the FRD solenoid-bottle-valve dispensers [32]. An example of the assay performance is shown in Fig. **4** that was plotted from an assay plate following transfer of DMSO (dimethyl sulfoxide) alone. For controls, the first two columns contained the positive control dexamethasone at a 0.1 μM final concentration. The S/B was 8.9 and Z' factor was 0.55, indicating a HTS-compatible assay. For the qHTS each compound was tested at between 7 and 15 concentration points (using a 1:5 or $1:\sqrt{5}$ dilution with the highest concen-
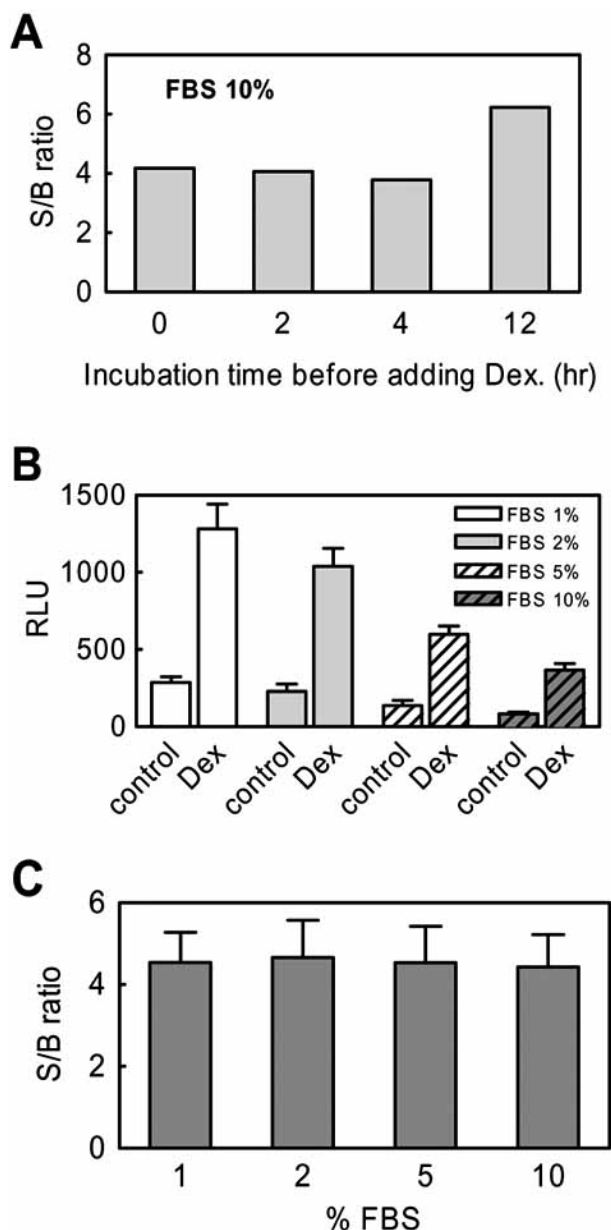
Fig. (2). Development of a wash-free assay in 1536-well format using fresh suspension cells. (A) Effect of incubation time before dexamethasone (Dex) addition on the S/B ratio. Effect of fetal bovine serum (FBS) on the chemiluminescence signal generated by β-galactosidase (**B**) and S/B ratio. (**C**) The data was averaged from 64 data points.

tration of 46 μM in the assay) and CR curves were generated for every compound in the 9,920 member validation collection (Table **2**). Systematic background patterns were eliminated by using DMSO blanks and lowest concentration plates to detect the assay background signature. In the 100 1536-well plate validation screen, 99 plates gave data suitable for analysis displaying an average robust (median-based) Z' of 0.43 (Fig. **4**) with an average S:B of 8.35.

To examine the activity of steroid-based compounds in the GR-EFC screen we classified the activity for all 197 steroids present in the compound collection. Of the 197 ster-
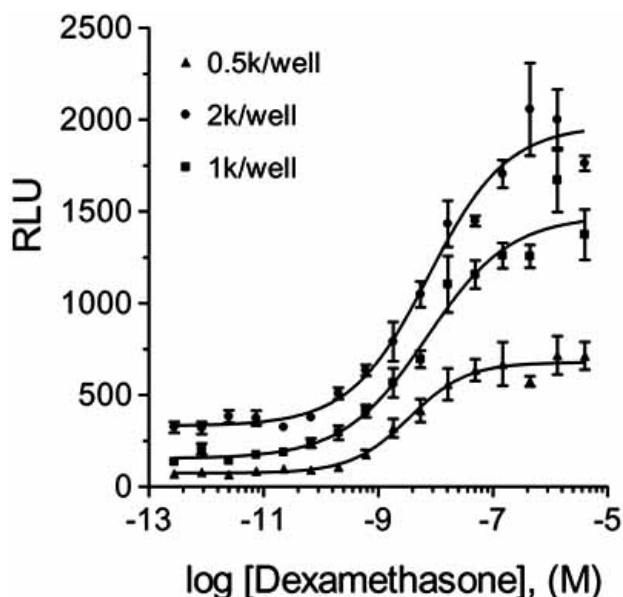
Fig. (3). Effect of cell density on dexamethasone-CR curves. For the fresh suspension cells, the EC_{50} values were 7.9, 15 and 7.8 nM for 0.5k, 1k and 2k per well, respectively. The titrations were plotted by the average of four data points. Dexamethasone was pin-tool transferred to 1536-well plates.
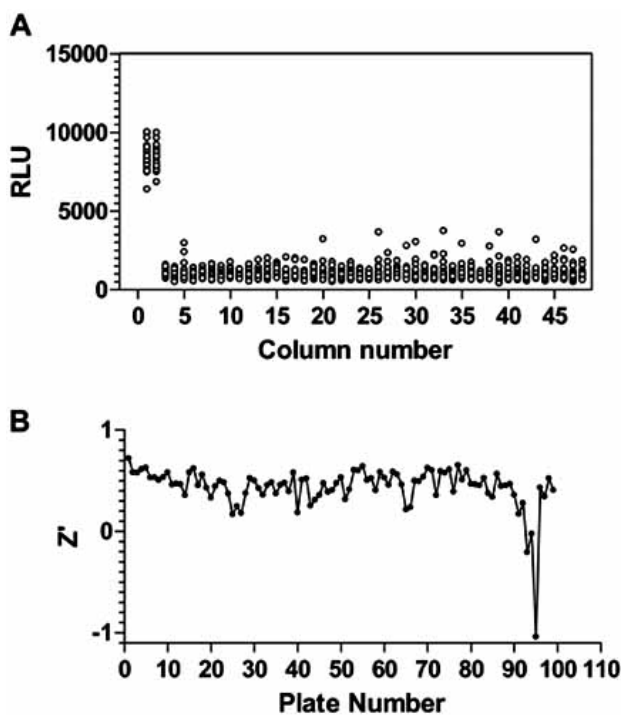
Fig. (4). 1536-well assay and performance. (**A**) Representative screening plate where compound field contains DMSO only. The screen was performed using 1536-white solid bottom plates. For controls, dexamethasone at 0.1 μM was present in column 1 and 2, while column 3 and 4 were DMSO alone and the remaining wells were used for compound testing. The S/B=8.9 and Z' factor=0.59. All wells contain the same amount of DMSO (30 nL). (**B**) Robust Z' analysis of 100 plate validation qHTS.

oid-like samples that were screened, 47 displayed agonist activity (Class 1 and 2, Appendix 1) and the remaining 150

were inactive (Class 4) A common active scaffold could be identified that described nearly 90% of the actives (41 of the 47 actives; see Fig. **5**). Inactive scaffolds were more diverse and four common scaffolds could be defined that covered 70% of the inactives (Fig. **5**).

Representative Class 1 curves corresponding to compounds annotated as glucocorticoids in bioactive collections such as LOPAC showed EC_{50} values < 100 nM for many, and all were < 1 μM (Fig. **5**). However, while all active steroids showed potent EC_{50} values (Class 1) large efficacy differences were observed for these in the qHTS. For example, the GR antagonist mifepristone, was present within the LOPAC library and displayed an EC_{50} of 2.2 nM with an efficacy of approximately 30%. As well, 17α-hydroprogesterone showed an EC_{50} of 730 nM and increased the luminescence signal only by approximately 30%. Additionally, some compounds were assayed more than once in the qHTS as samples were present from two different vendors (e.g., Prestwick and LOPAC). We noted that such inter-vendor duplicates often showed lower efficacy in the Prestwick library than samples in the LOPAC library (Fig. **6a,b**, dashed lines). However, the potency was measured at < 100 nM and therefore the qHTS approach identified these as Class 1 CR curves, although the response magnitude varied. The positive control dexamethasone was present in the Tocris library and showed a response that was in good agreement with the validation data for this assay (Fig. **6c**). Additionally, steroids that act as ligands to other nuclear receptors such as the estrogen receptor were found to be inactive (e.g., Class 4; Appendix 1).

Large scale HTS is most commonly performed using a single compound concentration. Therefore, to evaluate the performance of the assay with respect to a single screening concentration, we conducted a retrospective analysis of the qHTS data (Fig. **7a**) by examining single concentration datasets from the titration series in isolation (Table **3**). A representation of the 9 μM screening concentration is shown in Fig. **7b**. To perform the analysis we chose to compare positives above either 3σ or 6σ threshold values and asked how many of these compounds were associated with either Class 1 and 2, or Class 1 - 3 CR curves. In comparison to high confidence CR curves (Classes 1 and 2), the percentage of false positives was found to be approximately 1.3% using a 3σ threshold and approximately 0.3% using a 6σ threshold at either a 9 or 1.8 μM screening concentration. This indicates an accuracy of 98.7% for determining a true negative. However given the generally large size of compound libraries (e.g., 9,920 screened in this study), and the fact that the majority of compounds are inactive, even a false positive rate as low as 1% can result in a relatively large number of 'hits'. Therefore the confirmation of hits is greatly affected by small percentages of false positives. For example, for the assay evaluated here this leads to simulated confirmation rates of approximately 26% or 54% at a 3σ or 6σ threshold, respectively. Therefore for a library of 10K in size we would expect ~130 false positives (i.e., 98.7% accuracy). Note that the fraction of false positives does not depend on screening concentration as expected for stochastic events. Inclusion of the lower confidence CR curves (Class 3) results in a slight reduction in false positives at the 9 uM screening concentration (Table **3**). Overall, the assay accuracy observed here is in agreement with typical cell-based assays [37].
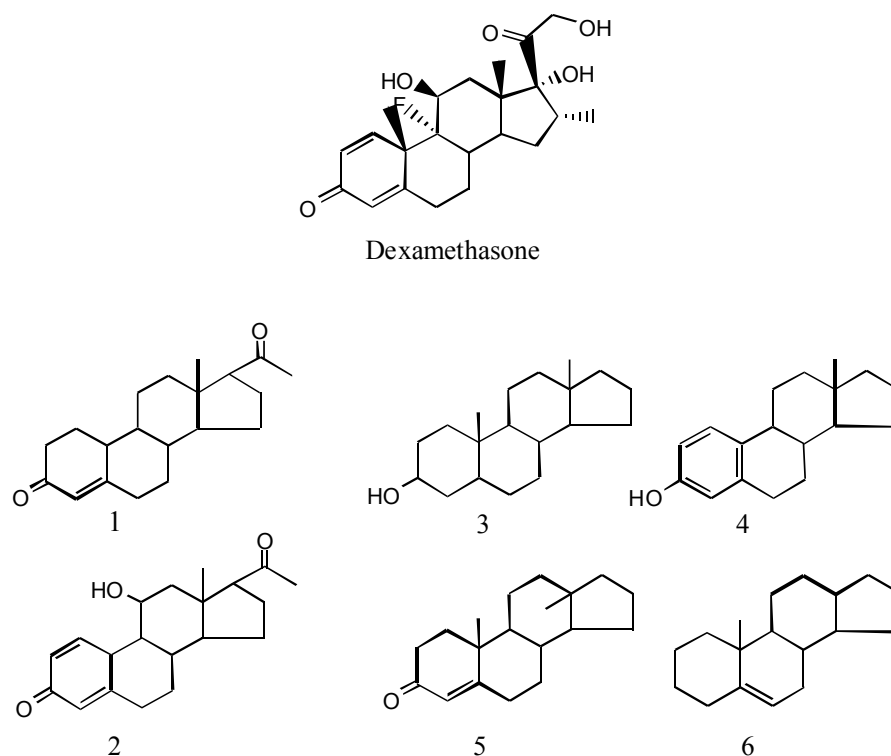
Dexamethasone

Fig. (5). Dexamethasone control, active and inactive steroid-based scaffolds identified in the qHTS. The active scaffold (1 and 2) covers all 41 of the 47 actives identified. Also shown are representative inactive scaffolds (3-6) that cover 105 of the 150 inactive steroidal compounds.
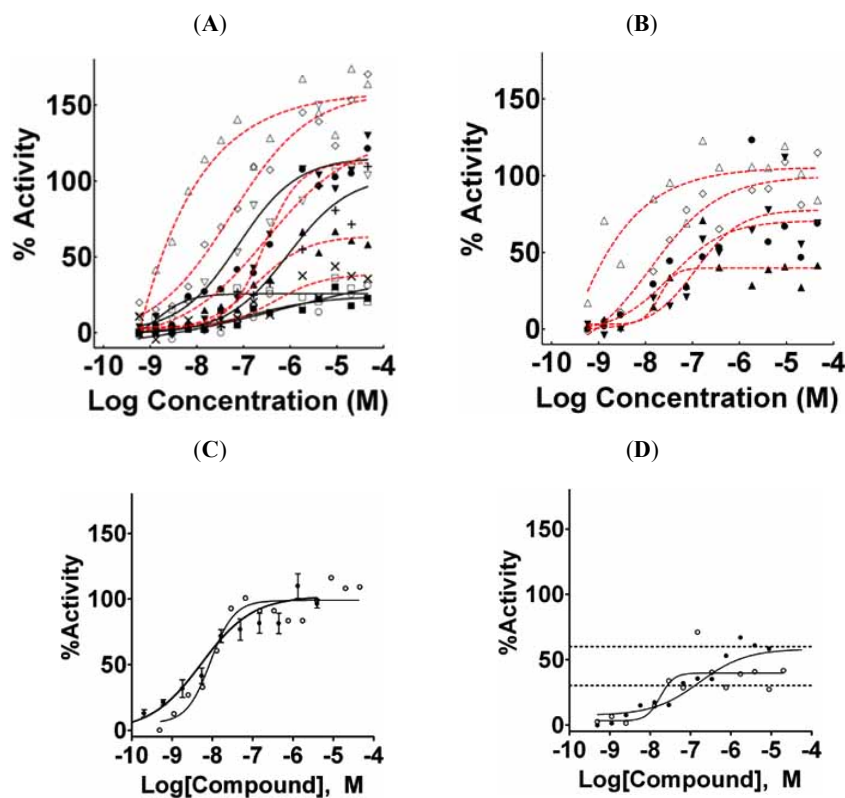
Fig. (6). Titration curves generated for representative glucocorticoids. (**A**) Representative glucocorticoids from the LOPAC collection. □, mifepristone; Δ, budesonide; upside-down open triangle, beclomethasone; ◊, betamethasone, ○, 17α-progesterone; ■, cyproterone acetate; ▲, corticosterone; ▼, triamcnolone; filled diamond, hydrocortisone, *, 11-deoxycortisol, +, hydrocortisone 21-hemisuccinate. Compounds that were also present in the Prestwick collection are shown with red-dashed fits. (**B**) CR curve data for compounds in the Prestwick collection. Symbols are as in A. (**C**) CR curves for dexamethasone from the validation (●) and the qHTS (○). (**D**) Example CR curves for corticosterone from LOPAC (●) and Prestwick (○). Plots were made by GraphPad Prism (San Diego, CA).
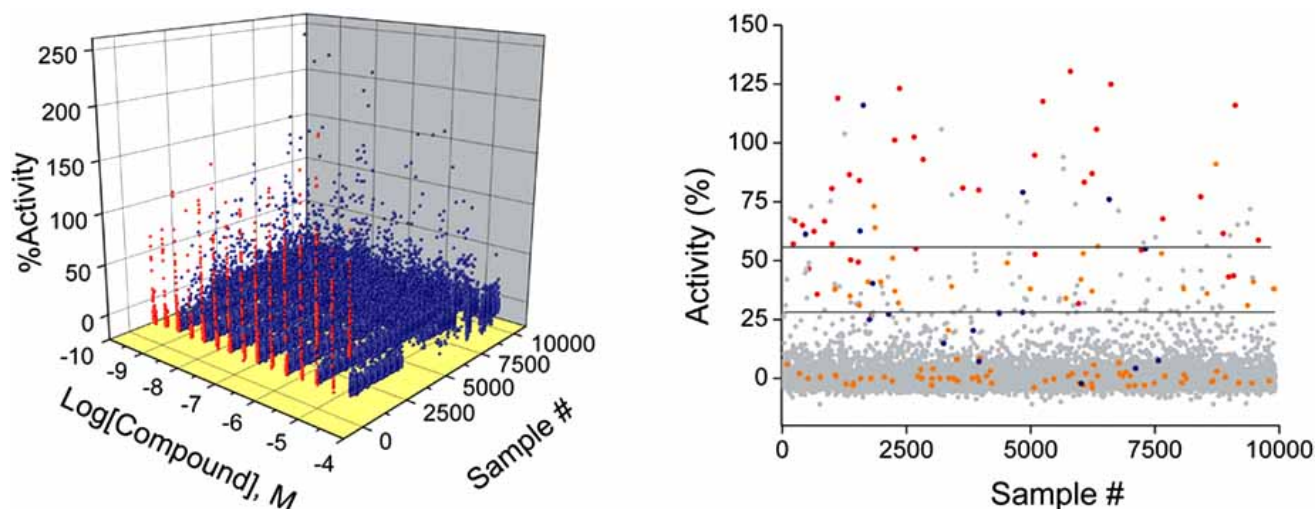
Fig. (7). qHTS and traditional HTS. (**A**) A 3D scatter plot of qHTS data lacking (blue) or showing (red) concentration-response relationships for all 9,920 samples screened. (**B**) A scatter plot of the 9 µM data with the data colored by the curve class as follows, Class 1 (red), Class 2 (blue), Class 3 (orange), and Class 4 inactive (grey). The thresholds for three and six SD are indicated as black lines.

Table 2.   Analysis of qHTS

IC$_{50}$ (uM)	Curve Classification					
	1a	**1b**	**2a**	**2b**	**3**	**Total**
<0.1	22	10	0	0	0	32
>0.1 to 1	3	3	1	2	0	9
>1 to 10	1	0	3	1	9	14
>10 to 100	0	0	0	7	28	35
>100	0	0	0	4	56	60
Total per classification	26	13	4	14	93	150
% library	0.26%	0.23%	0.04%	0.14%	0.93%	1.5%

As mentioned above many known glucocorticoids were identified using the qHTS approach despite large differences in efficacy between compounds and samples prepared by different vendors. However, to evaluate the sensitivity of the assay using the more common single-concentration-based HTS approach we examined the number of false negative glucocorticoids at two concentrations, 1.8 and 9 µM. This retrospective analysis is possible because of the comprehensive compound concentration range (0.5 nM to 46 µM; Table **1**) coverage by qHTS. Using a 3σ threshold we found the false negative rate to be approximately 12% but this increased to 33% when a 6σ threshold was used. One example of how true positives compounds can be missed using threshold values in HTS is illustrated in Fig. **6d**. Here a glucocorticoid from the Prestwick library shows low efficacy but high potency as determined by qHTS-derived CR curve. However the variation in the assay signal at the 9 µM point caused this data point to fall below the 3σ threshold. Meanwhile, the same compound from the LOPAC library is iden-

tified at 3σ but not at 6σ, again largely due to compound efficacy <100% of control values.

Table 3.   Summary of the Retrospective Analysis of the qHTS

9.2 uM	Threshold	TP	FP	FN	TN
Class 1-2	3 σ	50	129	7	9,735
	6 σ	38	31	19	9,833
Class 1-3	3 σ	76	103	NA	9,668
	6 σ	45	24	NA	9,747
1.8 uM	**Threshold**	**TP**	**FP**	**FN**	**TN**
Class 1-2	3 σ	40	131	NA	9,733
	6 σ	31	27	NA	9,837

TP: true positive; FP: false positive; FN: false negative; TN: true negative. NA: not applicable. Class 3 CR curves are relevant for this analysis when the 1.8 µM or 9 µM was the highest tested concentration as these curves are fit to a single point. However, all libraries were screened at a higher concentration then 1.8 µM and some were screened at higher than 9 µM and therefore the false negative numbers are found to be inflated when including this curve class. Therefore, for calculation of false negatives we only report the numbers using the high confidence curve classes. Also, note for this reason the TP and FP numbers are the same using Class 1-3 curve class as the comparison set for the 1.8 µM dataset.

DISCUSSION

The regulation of protein localization within cells is one of the fundamental mechanisms operating in signal transduction pathways. The application of EFC to measure GR nuclear localization yields an assay that allows monitoring protein translocation without the use of imaging microscopy technology. We desired to validate this assay in a 1536-well system and were able to optimize the assay using addition-only protocols that enabled a low volume assay with significant improvements in throughput.

The main advantage of using suspension cells is to reduce assay time. Here the use of suspension cells gives a sufficient assay window to perform the GR-EFC assay using the protocol in Table **1**. In addition, using suspension cells can reduce the assay cycle time by more than half, lowering the possibility of bacterial contamination that can occur during overnight culture. This was especially important for assay formats using antibiotic-free medium. As well, the use of suspension cells allowed for improved control of the cell density (cells/well) as the cells can be counted just prior to the assay. The optimized 1536-well GR-EFC assay showed good performance with a Z' score of 0.55. Comparison to a single concentration-based HTS showed that this cell-based assay possessed good accuracy with a false positive rate <1.4%.

The activity of the glucocorticoids in the GR-EFC assay supported the assay's biological relevance. While known GR ligands were detected with EC_{50} values in the nM range, compounds selective to other steroid receptors such as the estrogen receptor were inactive. Although literature values do not report detailed information on EC_{50}s for all the glucocorticoids screened here, we were able to compare IC_{50} values from binding studies with EC_{50} values from our current GR translocation assay in some cases. In the binding studies cited here, IC_{50} values were determined as the concentration of compound displacing 50% of [³H]-dexamethasone from specific GR binding. For example, EC_{50} values for dexamethasone, prednisolone and betamethasone in the current GR assay were all in agreement with the IC_{50} values found reported from previous studies [38-40]. Specifically, the IC_{50} for dexamethasone in a binding study was reported at 9.5 nM [38], compared to an EC_{50} value of 6 nM in the current study. Although the glucocorticoids showed potent EC_{50} values we noted a wide range of efficacy values (Fig. **6** and Table **4**). The qHTS approach improved the sensitivity of the assay such that low efficacy compounds that would be missed (i.e., false negative) at a single concentration using typical threshold cutoffs could be easily identified using the qHTS CR curves. Potent but low efficacy activities associated with steroids were also observed in a qHTS against a cell-based assay for IκBα stabilization (also see PubChem AID: 445) [41].

Table 4. EC_{50} Values from Representing Compounds

	EC_{50} (μM) (GR-EFC Assay)	IC_{50}/K_d (μM) [³H]dex Binding Assay
Dexamethasone	0.0060	0.0095 [38]
Betamethasone	0.057	0.025 [38]
17α-hydroxyprogesterone	2.87	n/a
Corticosterone	0.036	0.048 [39]
Predinisolone	0.066	0.10 [38]
Hydrocortisone	1.52	n/a
Budesonide	0.005	n/a
Mifepristone*	0.0022, 0.0013**	0.0015 [40]
Fluticasone propionate	0.0061	n/a

IC_{50}/K_d Values were derived from GR binding study using GR-rich cell extract.
* Mifepristone show only a 30% effect compared to Dexamethasone in this assay; ** independent re-test value with 25% efficacy.

Our results for mifepristone illustrate the potential for this kind of translocation assay to identify low efficacy actives. Mifepristone has been classified as an antagonist for the progesterone nuclear receptor and GR [42], but also observed to have GR agonist activity in some types of cells [43]. In the present study, the EC_{50} for mifepristone was 2.2 nM, but it produced only a 28% maximal increase in translocation activity which would act to antagonize the action of GR agonists such as dexamethasone. The reported reduction in dexamethasone-mediated GR translocation by mifepristone is consistent with findings that mifepristone does not affect the affinity of GR for DNA binding elements [44], rather it stabilizes GR with heat shock protein [45], leading to a reduction of nuclear translocation [46, 47] and would be consistent with partial 'agonist' activity demonstrated here. This provides an additional potential mode of action for antagonizing GR effects, which may be exploited in future drug development efforts.

SUMMARY

A novel cell-based assay using a 1536-well plate format was developed to screen 9,920 compounds at seven to fifteen concentrations (PubChem AID: 451). All GR ligands were detected with EC_{50} values in the nM range. The use of freshly prepared cell suspensions shortened the assay cycle time and was a critical to the optimization in a1536-well format. Our retrospective analysis using false positive occurrence as an indicator showed that the assay had good accuracy. As well, the assay demonstrated acceptable sensitivity as judged by the identification of the relevant glucocorticoids in the collection. Alterations in GR translocation may be responsible for glucocorticoid resistance, suggesting additional mechanisms by which to modulate GR activity [20, 21]. Thus, identifying non-steroidal small molecules which interfere with the GR translocation apparatus may have significant therapeutic value.

ACKNOWLEDGEMENTS

ABBREVIATIONS

CHO	=	Chinese hamster ovary
Dex	=	Dexamethasone
DMSO	=	Dimethyl sulfoxide
EFC	=	Enzymatic fragment complementation
GR	=	Glucocorticoid receptor
qHTS	=	Quantitative high throughput screening
S/B	=	Signal-to-background ratio
TP	=	True positive
FP	=	False positive
FN	=	False negative
TN	=	True negative

Appendix 1

Entry No.	Structure ID	Active Tag	Scaffold Class	qHTS Curve Class	qHTS Max Activity	qHTS Hill Slope	log qEC_{50}	qEC_{50} (M)	Supplier Name	Supplier Compound ID	Pub Chem SID
1	NCGC00016621-01	T	1	1.1			-11.23	5.90E-12	Prestwick	CAS-3093-35-4	11112527
2	NCGC00013661-01	T	1	1.1	90.0	0.65	-7.628	2.36E-08	NCI	NSC-53892	4253108
3	NCGC00015507-01	T	1	1.1	123.7	0.55	-6.498	3.18E-07	SigmaAldrich	Lopac-H-4001	11111268
4	NCGC00016153-01	T	1	1.1	100.0	0.62	-5.952	1.12E-06	SigmaAldrich	Lopac-H-2270	11112032
5	NCGC00016214-01	T	1	1.2	37.8	1.35	-7.782	1.65E-08	Prestwick	CAS-50-22-6	11112096
6	NCGC00016215-01	T	1	1.2	60.7	0.70	-7.579	2.63E-08	Prestwick	CAS-50-23-7	11112097
7	NCGC00016476-01	T	1	1.2	74.0	0.75	-6.953	1.11E-07	Prestwick	CAS-514-36-3	11112377
8	NCGC00015222-01	T	1	1.2	64.0	0.77	-6.747	1.79E-07	SigmaAldrich	Lopac-C-2505	11110926
9	NCGC00015886-01	T	1	1.2	41.2	0.59	-6.363	4.34E-07	SigmaAldrich	Lopac-R-0500	11111729
10	NCGC00016586-01	T	1	1.3	104.7	0.69	-7.725	1.88E-08	Prestwick	CAS-1524-88-5	11112491
11	NCGC00013220-01	T	1	2.2	100.0	0.54	-6.215	6.10E-07	NCI	NSC-17245	4252667
12	NCGC00013112-01	T	1	2.2	100.0	0.50	-6.147	7.12E-07	NCI	NSC-10483	4252559
13	NCGC00015785-01	T	1	2.2	100.0	0.38	-3.652	0.000223	SigmaAldrich	Lopac-P-0130	11111592
14	NCGC00015510-01	T	1	2.2	100.0	0.35	-3.42	0.00038	SigmaAldrich	Lopac-H-5752	11111272
15	NCGC00016616-01	T	1	2.4	100.0	0.13	-5.381	4.16E-06	Prestwick	CAS-2668-66-8	11112522
16	NCGC00013301-01	F	1	4		1.26	-3.035	0.000922	NCI	NSC-23904	4252748
17	NCGC00013824-01	F	1	4			-3.035	0.000922	NCI	NSC-75541	4253271
18	NCGC00013849-01	F	1	4			-3.035	0.000922	NCI	NSC-79103	4253296
19	NCGC00013931-01	F	1	4			-3.035	0.000922	NCI	NSC-88915	4253378
20	NCGC00014099-01	F	1	4			-3.035	0.000922	NCI	NSC-109131	4253546
21	NCGC00014152-01	F	1	4			-3.035	0.000922	NCI	NSC-114792	4253599
22	NCGC00016236-01	F	1	4			-2.686	0.002061	Prestwick	CAS-53-06-5	11112118
23	NCGC00016253-01	F	1	4			-2.686	0.002061	Prestwick	CAS-57-83-0	11112137
24	NCGC00016292-01	F	1	4			-2.686	0.002061	Prestwick	CAS-64-85-7	11112177
25	NCGC00015224-01	F	1	4			-2.336	0.004608	SigmaAldrich	Lopac-C-2755	11110928
26	NCGC00015228-01	F	1	4			-2.336	0.004608	SigmaAldrich	Lopac-C-3130	11110933
27	NCGC00016604-01	T	2	1.1		0.50	-11.23	5.90E-12	Prestwick	CAS-2135-17-3	11112510
28	NCGC00016788-01	T	2	1.1			-11.23	5.90E-12	Prestwick	CAS-25122-46-7	11112699
29	NCGC00016950-01	T	2	1.1			-11.23	5.90E-12	Prestwick	CAS-83919-23-7	11112866
30	NCGC00013438-01	T	2	1.1	85.0	0.79	-8.636	2.31E-09	NCI	NSC-37641	4252885
31	NCGC00015165-01	T	2	1.1	146.8	1.08	-8.312	4.87E-09	SigmaAldrich	Lopac-B-7777	11110860
32	NCGC00016442-01	T	2	1.1	84.0	0.63	-8.086	8.21E-09	Prestwick	CAS-426-13-1	11112339
33	NCGC00025017-01	T	2	1.1	99.4	1.27	-8.047	8.97E-09	Tocris	Tocris-1126	11113934
34	NCGC00016439-01	T	2	1.1	96.5	0.89	-7.634	2.33E-08	Prestwick	CAS-378-44-9	11112336
35	NCGC00016216-01	T	2	1.1	67.7	1.02	-7.53	2.95E-08	Prestwick	CAS-50-24-8	11112098
36	NCGC00015136-01	T	2	1.1	105.1	0.67	-7.278	5.27E-08	SigmaAldrich	Lopac-B-0385	11110827

(Appendix 1) contd…..

Entry No.	Structure ID	Active Tag	Scaffold Class	qHTS Curve Class	qHTS Max Activity	qHTS Hill Slope	log qEC50	qEC50 (M)	Supplier Name	Supplier Compound ID	Pub Chem SID
37	NCGC00015161-01	T	2	1.1	156.2	0.56	-7.25	5.62E-08	SigmaAldrich	Lopac-B-7005	11110856
38	NCGC00016822-01	T	2	1.1	80.7	0.44	-7.111	7.75E-08	Prestwick	CAS-33564-31-7	11112734
39	NCGC00016037-01	T	2	1.1	113.5	1.03	-6.563	2.73E-07	SigmaAldrich	Lopac-T-6376	11111903
40	NCGC00016330-01	T	2	1.2	63.5	0.98	-7.457	3.49E-08	Prestwick	CAS-83-43-2	11112219
41	NCGC00016566-01	T	2	1.2	64.9	1.69	-7.265	5.43E-08	Prestwick	CAS-1177-87-3	11112471
42	NCGC00016376-01	T	2	1.2	67.5	1.15	-7.082	8.27E-08	Prestwick	CAS-124-94-7	11112269
43	NCGC00016862-01	T	2	1.3	104.0	0.76	-8.701	1.99E-09	Prestwick	CAS-51333-22-3	11112776
44	NCGC00016856-01	T	2	1.3	77.5	0.52	-8.507	3.11E-09	Prestwick	CAS-49697-38-3	11112770
45	NCGC00016983-01	T	2	1.3	97.1	0.57	-8.315	4.85E-09	Prestwick	CAS-542449	11112899
46	NCGC00016990-01	T	2	1.3	64.5	1.18	-7.909	1.23E-08	Prestwick	CAS-1327543	11112906
47	NCGC00016433-01	T	2	1.3	80.8	0.52	-7.456	3.50E-08	Prestwick	CAS-338-98-7	11112330
48	NCGC00016824-01	T	2	1.4	53.9	0.52	-8.69	2.04E-09	Prestwick	CAS-34097-16-0	11112736
49	NCGC00016926-01	T	2	1.4	30.2	0.96	-8.025	9.44E-09	Prestwick	CAS-73771-04-7	11112841
50	NCGC00016436-01	T	2	1.4	47.0	-	-7.893	1.28E-08	Prestwick	CAS-356-12-7	11112333
51	NCGC00016984-01	T	2	2.1	100.0	0.34	-6.097	8.01E-07	Prestwick	CAS-667634-13-2	11112900
52	NCGC00013947-01	T	2	2.1	200.0	1.30	-5.5	3.16E-06	NCI	NSC-90616	4253394
53	NCGC00025343-01	T	Misc	1.1			-11.23	5.90E-12	Tocris	Tocris-2007	11114264
54	NCGC00016943-01	T	Misc	1.3	115.3	1.50	-9.43	3.72E-10	Prestwick	CAS-80474-14-2	11112859
55	NCGC00015700-01	T	Misc	1.4	25.5	2.07	-8.59	2.57E-09	SigmaAldrich	Lopac-M-8046	11111492
56	NCGC00016516-01	T	Misc	1.4	47.2	0.49	-7.254	5.57E-08	Prestwick	CAS-595-33-5	11112421
57	NCGC00013946-01	T	Misc	2.1	200.0	1.36	-5.133	7.37E-06	NCI	NSC-90615	4253393
58	NCGC00025179-01	T	Misc	2.4	100.0	2.34	-4.408	3.91E-05	Tocris	Tocris-1479	11114100
59	NCGC00013010-01	F	3	4			-3.035	0.000922	NCI	NSC-1614	4252457
60	NCGC00013092-01	F	3	4			-3.035	0.000922	NCI	NSC-8797	4252539
61	NCGC00013426-01	F	3	4			-3.035	0.000922	NCI	NSC-36819	4252873
62	NCGC00013541-01	F	3	4			-3.035	0.000922	NCI	NSC-45236	4252988
63	NCGC00013657-01	F	3	4			-3.035	0.000922	NCI	NSC-53396	4253104
64	NCGC00013708-01	F	3	4			-3.035	0.000922	NCI	NSC-59276	4253155
65	NCGC00013713-01	F	3	4			-3.035	0.000922	NCI	NSC-59620	4253160
66	NCGC00013740-01	F	3	4			-3.035	0.000922	NCI	NSC-63558	4253187
67	NCGC00013804-01	F	3	4			-3.035	0.000922	NCI	NSC-73109	4253251
68	NCGC00013865-01	F	3	4			-3.035	0.000922	NCI	NSC-82802	4253312
69	NCGC00013974-01	F	3	4			-3.035	0.000922	NCI	NSC-93241	4253421
70	NCGC00014098-01	F	3	4			-3.035	0.000922	NCI	NSC-109128	4253545
71	NCGC00014902-01	F	3	4			-3.035	0.000922	NCI	NSC-407807	4254349
72	NCGC00014987-01	F	3	4			-3.035	0.000922	NCI	NSC-683770	4254434

Entry No.	Structure ID	Active Tag	Scaffold Class	qHTS Curve Class	qHTS Max Activity	qHTS Hill Slope	log qEC50	qEC50 (M)	Supplier Name	Supplier Compound ID	Pub Chem SID
73	NCGC00016238-01	F	3	4			-2.686	0.002061	Prestwick	CAS-53-41-8	11112120
74	NCGC00016238-02	F	3	4			-2.686	0.002061	Prestwick	CAS-53-42-9	11112121
75	NCGC00016238-03	F	3	4			-2.686	0.002061	Prestwick	CAS-481-29-8	11112122
76	NCGC00016295-01	F	3	4			-2.686	0.002061	Prestwick	CAS-66-28-4	11112183
77	NCGC00016319-01	F	3	4			-2.686	0.002061	Prestwick	CAS-77-59-8	11112208
78	NCGC00016387-01	F	3	4			-2.686	0.002061	Prestwick	CAS-128-13-2	11112280
79	NCGC00016387-02	F	3	4			-2.686	0.002061	Prestwick	CAS-474-25-9	11112281
80	NCGC00016406-01	F	3	4			-2.686	0.002061	Prestwick	CAS-143-62-4	11112300
81	NCGC00016445-01	F	3	4			-2.686	0.002061	Prestwick	CAS-434-13-9	11112342
82	NCGC00016448-01	F	3	4			-2.686	0.002061	Prestwick	CAS-467-55-0	11112345
83	NCGC00016452-01	F	3	4			-2.686	0.002061	Prestwick	CAS-475-31-0	11112349
84	NCGC00016524-01	F	3	4			-2.686	0.002061	Prestwick	CAS-630-64-8	11112429
85	NCGC00016591-01	F	3	4			-2.686	0.002061	Prestwick	CAS-1672-46-4	11112497
86	NCGC00016716-01	F	3	4			-2.686	0.002061	Prestwick	CAS-15500-66-0	11112624
87	NCGC00016782-01	F	3	4			-2.686	0.002061	Prestwick	CAS-23930-19-0	11112692
88	NCGC00016783-01	F	3	4			-2.686	0.002061	Prestwick	CAS-23930-37-2	11112693
89	NCGC00017076-01	F	3	4			-2.686	0.002061	Prestwick	CAS-11018-89-6	11112992
90	NCGC00015090-01	F	3	4			-2.336	0.004608	SigmaAldrich	Lopac-A-7755	11110776
91	NCGC00015112-01	F	3	4			-2.336	0.004608	SigmaAldrich	Lopac-A-9755	11110802
92	NCGC00015804-01	F	3	4			-2.336	0.004608	SigmaAldrich	Lopac-P-1918	11111617
93	NCGC00015805-01	F	3	4			-2.336	0.004608	SigmaAldrich	Lopac-P-2016	11111618
94	NCGC00015820-01	F	3	4			-2.336	0.004608	SigmaAldrich	Lopac-P-5052	11111636
95	NCGC00015853-01	F	3	4			-2.336	0.004608	SigmaAldrich	Lopac-P-8887	11111682
96	NCGC00016061-01	F	3	4			-2.336	0.004608	SigmaAldrich	Lopac-T-9034	11111930
97	NCGC00017282-01	F	3	4			-2.336	0.004608	Timtec	TNP00197	11113200
98	NCGC00017309-01	F	3	4			-2.336	0.004608	Timtec	TNP00235	11113227
99	NCGC00024736-01	F	3	4			-2.336	0.004608	Tocris	Tocris-0693	11113650
100	NCGC00013034-01	F	4	4			-3.035	0.000922	NCI	NSC-3354	4252481
101	NCGC00013235-01	F	4	4			-3.035	0.000922	NCI	NSC-18312	4252682
102	NCGC00013236-01	F	4	4			-3.035	0.000922	NCI	NSC-18320	4252683
103	NCGC00013333-01	F	4	4			-3.035	0.000922	NCI	NSC-26645	4252780
104	NCGC00013908-01	F	4	4			-3.035	0.000922	NCI	NSC-86467	4253355
105	NCGC00014013-01	F	4	4			-3.035	0.000922	NCI	NSC-97845	4253460
106	NCGC00014107-01	F	4	4			-3.035	0.000922	NCI	NSC-109509	4253554
107	NCGC00014125-01	F	4	4			-3.035	0.000922	NCI	NSC-112737	4253572
108	NCGC00017797-01	F	4	4			-3.035	0.000922	BUCMLD	BUCMLD-JRG-1-179	

(Appendix 1) contd…..

Entry No.	Structure ID	Active Tag	Scaffold Class	qHTS Curve Class	qHTS Max Activity	qHTS Hill Slope	log qEC50	qEC50 (M)	Supplier Name	Supplier Compound ID	Pub Chem SID
109	NCGC00016217-01	F	4	4			-2.686	0.002061	Prestwick	CAS-50-27-1	11112099
110	NCGC00016218-01	F	4	4			-2.686	0.002061	Prestwick	CAS-50-28-2	11112100
111	NCGC00016237-01	F	4	4			-2.686	0.002061	Prestwick	CAS-53-16-7	11112119
112	NCGC00016310-01	F	4	4			-2.686	0.002061	Prestwick	CAS-72-33-3	11112199
113	NCGC00016682-01	F	4	4			-2.686	0.002061	Prestwick	CAS-7280-37-7	11112590
114	NCGC00015422-01	F	4	4			-2.336	0.004608	SigmaAldrich	Lopac-E-8875	11111161
115	NCGC00015423-01	F	4	4			-2.336	0.004608	SigmaAldrich	Lopac-E-9750	11111162
116	NCGC00015690-01	F	4	4			-2.336	0.004608	SigmaAldrich	Lopac-M-6383	11111479
117	NCGC00016078-01	F	4	4			-2.336	0.004608	SigmaAldrich	Lopac-U-6756	11111950
118	NCGC00024964-01	F	4	4			-2.336	0.004608	Tocris	Tocris-1047	11113880
119	NCGC00025091-01	F	4	4			-2.336	0.004608	Tocris	Tocris-1268	11114009
120	NCGC00025300-01	F	4	4			-2.336	0.004608	Tocris	Tocris-1807	11114221
121	NCGC00016444-01	F	5	4	15.2	0.97	-7.266	5.43E-08	Prestwick	CAS-434-03-7	11112341
122	NCGC00013637-01	F	5	4			-3.035	0.000922	NCI	NSC-51182	4253084
123	NCGC00013978-01	F	5	4			-3.035	0.000922	NCI	NSC-93354	4253425
124	NCGC00013979-01	F	5	4			-3.035	0.000922	NCI	NSC-93355	4253426
125	NCGC00016231-01	F	5	4			-2.686	0.002061	Prestwick	CAS-52-01-7	11112113
126	NCGC00016254-01	F	5	4			-2.686	0.002061	Prestwick	CAS-57-85-2	11112138
127	NCGC00016440-01	F	5	4			-2.686	0.002061	Prestwick	CAS-382-45-6	11112337
128	NCGC00015070-01	F	5	4			-2.336	0.004608	SigmaAldrich	Lopac-A-5791	11110752
129	NCGC00015109-01	F	5	4			-2.336	0.004608	SigmaAldrich	Lopac-A-9630	11110799
130	NCGC00015474-01	F	5	4			-2.336	0.004608	SigmaAldrich	Lopac-G-5168	11111228
131	NCGC00015948-01	F	5	4			-2.336	0.004608	SigmaAldrich	Lopac-S-3378	11111798
132	NCGC00025253-01	F	5	4			-2.336	0.004608	Tocris	Tocris-1672	11114174
133	NCGC00013542-01	F	6	4			-3.035	0.000922	NCI	NSC-45238	4252989
134	NCGC00013601-01	F	6	4			-3.035	0.000922	NCI	NSC-48630	4253048
135	NCGC00013669-01	F	6	4			-3.035	0.000922	NCI	NSC-54340	4253116
136	NCGC00013726-01	F	6	4			-3.035	0.000922	NCI	NSC-62349	4253173
137	NCGC00013777-01	F	6	4			-3.035	0.000922	NCI	NSC-69298	4253224
138	NCGC00013779-01	F	6	4			-3.035	0.000922	NCI	NSC-69540	4253226
139	NCGC00013830-01	F	6	4			-3.035	0.000922	NCI	NSC-76026	4253277
140	NCGC00013866-01	F	6	4			-3.035	0.000922	NCI	NSC-82803	4253313
141	NCGC00014002-01	F	6	4			-3.035	0.000922	NCI	NSC-96021	4253449
142	NCGC00014519-01	F	6	4			-3.035	0.000922	NCI	NSC-179187	4253966
143	NCGC00016331-01	F	6	4			-2.686	0.002061	Prestwick	CAS-83-46-5	11112220
144	NCGC00016381-01	F	6	4			-2.686	0.002061	Prestwick	CAS-126-17-0	11112274
145	NCGC00016409-01	F	6	4			-2.686	0.002061	Prestwick	CAS-145-13-1	11112303

(Appendix 1) contd…..

Entry No.	Structure ID	Active Tag	Scaffold Class	qHTS Curve Class	qHTS Max Activity	qHTS Hill Slope	log qEC50	qEC50 (M)	Supplier Name	Supplier Compound ID	Pub Chem SID
146	NCGC00016502-01	F	6	4			-2.686	0.002061	Prestwick	CAS-546-06-5	11112407
147	NCGC00016544-01	F	6	4			-2.686	0.002061	Prestwick	CAS-853-23-6	11112449
148	NCGC00015341-01	F	6	4			-2.336	0.004608	SigmaAldrich	Lopac-D-4000	11111068
149	NCGC00016143-01	F	6	4			-2.336	0.004608	SigmaAldrich	Lopac-D-5297	11112022
150	NCGC00016184-01	F	6	4			-2.336	0.004608	SigmaAldrich	Lopac-P-162	11112065
151	NCGC00017170-01	F	6	4			-2.336	0.004608	Timtec	TNP00027	11113086
152	NCGC00025241-01	F	6	4			-2.336	0.004608	Tocris	Tocris-1638	11114162
153	NCGC00016884-01	F	Misc	4	15.6	0.57	-6.634	2.32E-07	Prestwick	CAS-58652-20-3	11112799
154	NCGC00013099-01	F	Misc	4			-3.035	0.000922	NCI	NSC-9746	4252546
155	NCGC00013199-01	F	Misc	4			-3.035	0.000922	NCI	NSC-15520	4252646
156	NCGC00013292-01	F	Misc	4			-3.035	0.000922	NCI	NSC-23159	4252739
157	NCGC00013302-01	F	Misc	4			-3.035	0.000922	NCI	NSC-23922	4252749
158	NCGC00013585-01	F	Misc	4			-3.035	0.000922	NCI	NSC-48010	4253032
159	NCGC00013734-01	F	Misc	4			-3.035	0.000922	NCI	NSC-62791	4253181
160	NCGC00013793-01	F	Misc	4			-3.035	0.000922	NCI	NSC-72254	4253240
161	NCGC00013902-01	F	Misc	4			-3.035	0.000922	NCI	NSC-86008	4253349
162	NCGC00013920-01	F	Misc	4			-3.035	0.000922	NCI	NSC-88135	4253367
163	NCGC00014231-01	F	Misc	4			-3.035	0.000922	NCI	NSC-121137	4253678
164	NCGC00014911-01	F	Misc	4			-3.035	0.000922	NCI	NSC-521777	4254358
165	NCGC00016233-01	F	Misc	4			-2.686	0.002061	Prestwick	CAS-52-76-6	11112115
166	NCGC00016235-01	F	Misc	4			-2.686	0.002061	Prestwick	CAS-53-03-2	11112117
167	NCGC00016303-01	F	Misc	4			-2.686	0.002061	Prestwick	CAS-68-22-4	11112191
168	NCGC00016304-01	F	Misc	4			-2.686	0.002061	Prestwick	CAS-68-23-5	11112192
169	NCGC00016318-01	F	Misc	4			-2.686	0.002061	Prestwick	CAS-77-52-1	11112207
170	NCGC00016413-01	F	Misc	4			-2.686	0.002061	Prestwick	CAS-152-62-5	11112307
171	NCGC00016417-01	F	Misc	4			-2.686	0.002061	Prestwick	CAS-297-76-7	11112312
172	NCGC00016443-01	F	Misc	4			-2.686	0.002061	Prestwick	CAS-427-51-0	11112340
173	NCGC00016447-01	F	Misc	4			-2.686	0.002061	Prestwick	CAS-466-06-8	11112344
174	NCGC00016449-01	F	Misc	4			-2.686	0.002061	Prestwick	CAS-472-15-1	11112346
175	NCGC00016450-01	F	Misc	4			-2.686	0.002061	Prestwick	CAS-473-98-3	11112347
176	NCGC00016451-01	F	Misc	4			-2.686	0.002061	Prestwick	CAS-474-86-2	11112348
177	NCGC00016540-01	F	Misc	4			-2.686	0.002061	Prestwick	CAS-797-63-7	11112445
178	NCGC00016609-01	F	Misc	4			-2.686	0.002061	Prestwick	CAS-2363-58-8	11112515
179	NCGC00016726-01	F	Misc	4			-2.686	0.002061	Prestwick	CAS-17230-88-5	11112635
180	NCGC00016952-01	F	Misc	4			-2.686	0.002061	Prestwick	CAS-84371-65-3	11112868
181	NCGC00017016-01	F	Misc	4			-2.686	0.002061	Prestwick	CAS-81-23-2	11112932
182	NCGC00017030-01	F	Misc	4			-2.686	0.002061	Prestwick	CAS-751-94-0	11112946
183	NCGC00017073-01	F	Misc	4			-2.686	0.002061	Prestwick	CAS-7421-40-1	11112989

Entry No.	Structure ID	Active Tag	Scaffold Class	qHTS Curve Class	qHTS Max Activity	qHTS Hill Slope	log qEC50	qEC50 (M)	Supplier Name	Supplier Compound ID	Pub Chem SID
184	NCGC00017146-01	F	Misc	4			-2.686	0.002061	Prestwick	CAS-102731	11113062
185	NCGC00015230-01	F	Misc	4	40.0	0.28	-2.336	0.004608	SigmaAldrich	Lopac-C-3412	11110935
186	NCGC00015375-01	F	Misc	4			-2.336	0.004608	SigmaAldrich	Lopac-D-8399	11111105
187	NCGC00015377-01	F	Misc	4			-2.336	0.004608	SigmaAldrich	Lopac-D-8690	11111107
188	NCGC00016076-01	F	Misc	4			-2.336	0.004608	SigmaAldrich	Lopac-U-5882	11111948
189	NCGC00016090-01	F	Misc	4			-2.336	0.004608	SigmaAldrich	Lopac-W-104	11111962
190	NCGC00016148-01	F	Misc	4			-2.336	0.004608	SigmaAldrich	Lopac-F-0881	11112027
191	NCGC00017165-01	F	Misc	4			-2.336	0.004608	Timtec	TNP00020	11113081
192	NCGC00017222-01	F	Misc	4			-2.336	0.004608	Timtec	TNP00102	11113139
193	NCGC00017223-01	F	Misc	4			-2.336	0.004608	Timtec	TNP00103	11113140
194	NCGC00017244-01	F	Misc	4			-2.336	0.004608	Timtec	TNP00130	11113161
195	NCGC00017307-01	F	Misc	4			-2.336	0.004608	Timtec	TNP00233	11113225
196	NCGC00017359-01	F	Misc	4			-2.336	0.004608	Timtec	TNP00303	11113278
197	NCGC00024732-01	F	Misc	4			-2.336	0.004608	Tocris	Tocris-0687	11113646

REFERENCES

[1]   Beato, M.; Herrlich, P.; Schutz, G. *Cell,* **1995**, *83*, 851-857.
[2]   Mangelsdorf, D.J.; Thummel, C.; Beato, M.; Herrlich, P.; Schütz, G.; Umesono, K.; Blumberg, B.; Kastner, P.; Mark, M.; Chambon, P.; Evans, R.M. *Cell,* **1995**, *83,* 835-839.
[3]   Karin, M. *Cell,* **1998**, *93,* 487-490.
[4]   Adcock, I.M.; Caramori, G. *Immunol. Cell Biol.,* **2001**, *79*, 376-384.
[5]   Bia, C.; Schmidt, A.; Freedman. L.P. *Assay Drug Devel. Technol.,* **2003**, *1*, 843-852.
[6]   Barnes, P.J. *Clin. Sci. (Lond.),* **1998**, *94,* 557-572.
[7]   Herr, I.; Pfitzenmaier, J. *Lancet Oncol.,* **2006**, *7*, 425-430.
[8]   Pui, C.H.; Evans, W.E. *N. Engl. J. Med.,* **2006**, *354*, 166-178.
[9]   Inglese, J.; Johnson, R.L.; Simeonov, A.; Xia, M.; Zheng, W.; Austin, C.P.; Auld, D.S. *Nat. Chem. Biol.,* **2007**, *3*, 466-479.
[10] Udenfriend, S.; Gerber, L.D.; Brink, L. *Proc. Natl. Acad. Sci. USA,* **1985**, *82*, 8672-8676.
[11] Bosworth, N.; Towers, P. *Nature,* **1989**, *341*, 167-168.
[12] Lin, S.; Bock, C.L.; Gardner, D.B.; Webster, J.C.; Favata, M.F.; Trzaskos, J.M.; Oldenburg, K.R. *Anal. Biochem.,* **2002**, *300*, 15-21.
[13] Necela, B.M.; Cidlowski, J.A. *Steroids,* **2003**, *68*, 341-350.
[14] Willemsen, P.; Scippo, M.-L.; Kausel, G.; Figueroa, J.; Maghuin-Register, G.; Martial, J.A.; Muller, M. *Anal. Bioanal. Chem.,* **2004**, *378*, 655-663.
[15] Cadepond, F.; Schweizer-Groyer, G.; Segard-Maurel, I.; Jibard, N.; Hollenberg, S.M.; Giguère, V.; Evans, R.M.; Baulieu, E.E. *J. Biol. Chem.,* **1991**, *266*, 5834-5841.
[16] Richter, K.; Buchner, J. *J. Cell. Physiol.,* **2001**, *188*, 281-290.
[17] Lambert, J.R.; Nordeen, S.K. *J. Biol. Chem.,* **1998**, *273*, 32708-32714.
[18] Ito, K.; Barnes, P.J.; Adcock, I.M. *Mol. Cell. Biol.,* **2000**, *20*, 6891-6903.
[19] Kovacs, J.J.; Murphy, P.J.; Gaillard, S.; Zhao, X.; Wu, J.T.; Nicchitta, C.V.; Yoshida, M.; Toft, D.O.; Pratt, W.B.; Yao, T.P. *Mol. Cell,* **2005**, *18*, 601-607.
[20] Ito, K.; Yamamura, S.; Essilfie-Quaye, S.; Cosio, B.; Ito, M.; Barnes, P.J.; Adcock, I.M. *J. Exp. Med.,* **2006**, *203*, 7-13.
[21] Matthews, J.G.; Ito, K.; Barnes, P.J.; Adcock, I.M. *J. Allergy Clin. Immunol.,* **2004**, *113*, 1100-1108.
[22] Inglese, J. (ed.) Measuring Biological Responses with Automated Microscopy, Vol. *414.* (Elsevier Acadmeic Press, San Diego; **2006**).
[23] Taylor, D.L.; Haskins, J.R.; Giuliano, K.A. (eds.) High Content Screening, Vol. *356.* (Humana Press, **2006**).
[24] Auld, D.S. *et al. Methods Enzymol.,* **2006**, *414*, 566-589.
[25] Baens, M.; Noels, H.; Broeckx, V.; Hagens, S.; Fevery, S.; Billiau, A.D.; Vankelecom, H.; Marynen, P. *PLoS ONE,* **2006**, *1*, e54.
[26] Fung, P.; Peng, K.; Kobel, P.; Dotimas, H.; Kauffman, L.; Olson, K.; Eglen, R.M. *Assay Drug Dev. Technol.,* **2006**, *4*, 263-272.
[27] Wehrman, T.S.; Casipit, C.L.; Gewertz, N.M.; Blau, H.M. *Nat. Methods,* **2005**, *2*, 521-527.
[28] Eglen, R.M. *Assay Drug. Devel. Technol.,* **2002**, *1*, 97-104.
[29] Kalderon, D.; Roberts, B.L.; Richardson, W.D.; Smith, A.E. *Cell,* **1984**, *39*, 499-509.
[30] Saphire, A.C.; Bark, S.J.; Gerace, L. *J. Biol. Chem.,* **1998**, *273*, 29764-29769.
[31] Inglese, J.; Auld, D.S.; Jadhav, A.; Johnson, R.L.; Simeonov, A.; Yasgar, A.; Zheng, W.; Austin, C.P. *Proc. Natl. Acad. Sci. USA,* **2006**, *103*, 11473-11478.
[32] Niles, W.D.; Coassin, P.J. *Assay Drug. Devel. Technol.,* **2005**, *3*, 189-202 (2005).
[33] Cleveland, P.H. & Koutz, P.J. *Assay Drug Dev. Technol.,* **2005**, *3*, 213-225.
[34] Zhang, J.H.; Chung, T.D.; Oldenburg, K.R. *J. Biomol. Screen.,* **1999**, *4*, 67-73.
[35] Peterson, W.W. *IRE Trans. Inform. Theory*, **1954**, *4*, 171-212.
[36] Swets, J.A. *Science,* **1988**, *240*, 1285–1293.
[37] Gribbon, P.; Lyons, R.; Laflin, P.; Bradley, J.; Chambers, C.; Williams, B.S.; Keighley, W.; Sewing, A. *J. Biomol. Screen.,* **2005**, *10*, 99-107.
[38] Hammer, S.; Spika, I.; Sippl, W.; Jessen, G.; Kleuser, B.; Holtje, H.D.; Schafer-Korting, M. *Steroids,* **2003**, *68,* 329-339.

[39]   Lin, S.; Bzock, C.L.; Gardner, D.B.; Webster, J.C.; Favata, M.F.; Trzaskos, J.M.; Oldenburg, K.R. *Anal. Biochem.,* **2002**, *300*, 15-21.

[40]   Gagne, D.; Pons, M.; de Paulet, C. *J. Steroid Biochem.,* **1986**, *25,* 315-322.

[41]   Davis, R.E.; Zhang, Y.Q.; Southall, N.; Staudt, L.M.; Austin, C.P.; Inglese, J.; Auld, D.S. *Assay Drug Dev. Technol.,* **2007**, *5*, 85-103.

[42]   Spitz, I.M.; Bardin, C.W. *N. Engl. J. Med.,* **1993**, *329*, 404-412.

[43]   Zhang, S.; Jonklaas, J.; Danielsen, M. *Steroids,* **2007**, *72*, 600-8.

[44]   Pandit, S.; Geissler, W.; Harris, G.; Sitlani, A. *J. Biol. Chem.,* **2002**, *277*, 1538-1548.

[45]   Groyer, A.; Schweizer-Groyer, G.; Cadepond, F.; Mariller, M.; Baulieu, E.E. *Nature,* **1987**, *327*,624-626.

[46]   Moguilewsky, M.; Philibert, D. *J. Steroid Biochem.,* **1984**, *20*, 271-276.

[47]   Distelhorst, C.W.; Howard, K.J. *J. Steroid Biochem.,* **1990**, *36*, 25-31.